CHINESE JOURNAL OF MECHANICAL ENGINEERING
Vol. 27, No. 1, 2014

DOI: 10.3901/CJME.2014.01.122, available online at www.springerlink.com; www.cjmenet.com; www.cjmenet.com.cn

Pseudo-rigid-body Model for Corrugated Cantilever Beam Used in Compliant Mechanisms

WANG Nianfeng[1, 2, *], LIANG Xiaohe[1], and ZHANG Xianmin[1, *]

1 *Guangdong Province Key Laboratory of Precision Equipment and Manufacturing Technology, South China University of Technology, Guangzhou 510641, China*
2 *State Key Laboratory of Mechanical System and Vibration, Shanghai Jiao Tong University, Shanghai 200240, China*

Received March 21, 2013; revised September 9, 2013; accepted November 4, 2013

Abstract: Common compliant joints generally have limited range of motion, reduced fatigue life and high stress concentration. To overcome these shortcomings, periodically corrugated cantilever beam is applied to design compliant joints. Basic corrugated beam unit is modeled by using pseudo-rigid-body method. The trajectory and deformation behavior of periodically corrugated cantilever beam are estimated by the transformation of coordinate and superposition of the deformation of corrugated beam units. Finite element analysis(FEA) is carried out on corrugated cantilever beam to estimate the accuracy of the pseudo-rigid-body model. Results show that the kinetostatic behaviors obtained by this method, which has a relative error less than 6%, has good applicability and corrugated cantilever beam has the characteristics of a large range of motion and high mechanical strength. The corrugated cantilever beam is then applied to design a flexible rotational joint to obtain a larger angle output. The paper proposes a pseudo-rigid-body model for corrugated cantilever beam and designed a flexible rotational joint with large angle output.

Keywords: corrugated beam, pseudo rigid body method, compliant mechanisms

1 Introduction

Compliant mechanisms are flexible structures that deliver a desired motion by undergoing elastic deformation, as opposed to the rigid body motions of conventional mechanisms. Like a rigid-body mechanism, a compliant mechanism also transfers force and/or energy from a source to an output. Unlike rigid-link mechanisms, compliant mechanisms gain at least some of their mobility through the deflection of flexible members instead of through rigid links and movable joints. When compliance is included as a preferred effect, they offer distinct advantages over conventional rigid-link mechanisms especially when the applications are in the micro-dimensional scale. Advantages of compliant mechanisms include: easier to manufacture; more compact; elimination of joint friction, need for lubrication, and backlash due to joint clearances; materials friendly; can efficiently take advantage of modern actuators; can create motions for shape changing structures not possible with conventional "rigid" devices. Compared to rigid-body counterparts, compliant mechanisms have so many advantages and so can be created as a replacement of them. Practically, the applications of compliant mechanisms are unlimited, both in the macro domain and micro domain, for instance, for high precision manipulation stages, instruments for minimally invasive surgery, and micro-electro-mechanical systems(MEMS). And compliant mechanisms are a revolutionary impact and change to mechanical science and engineering [1–4].

Compliant mechanisms can provide distinct advantages over conventional rigid-body mechanisms, but including compliance complicates the design process. There has been a growing interest in the area of systematic approaches in compliant mechanism synthesis. Two main approaches have been developed for systematic synthesis and design of compliant mechanisms, a pseudo-rigid-body(PRB) approach and a topology optimization approach[5–12]. In PRB approach, compliant segments are modeled by several rigid links connected together by pin joints and torsional springs. Where to place the pin joints and springs to the model and the spring constants are calculated according to types of segments. Thus, the approach connects compliant mechanism directly to rigid-body mechanism theory. Today, this approach has been widely applied to design grippers[13], multistable mechanisms[14–15], compliant mechanisms for commercial products[16], microleverage mechanisms[17] and serial-chain open-loop compliant systems[18].

The flexible joints design is the crucial part of design

* Corresponding author. E-mail: menfwang@scut.edu.cn, zhangxm@scut.edu.cn

This project is supported by National Natural Science Foundation of China (Grant Nos. 51205134, 91223201), Doctoral Fund of Ministry of Education of China (Grant No. 20120172120001), Research Project of State Key Laboratory of Mechanical System and Vibration of China (Grant No. MSV201405), Guangdong Province Universities and Colleges Pearl River Scholar Funded Scheme (GDUPS, 2010), and Fundamental Research Funds for the Central Universities (Grant No. 2013ZM012)

based on PRB approach. Many flexible joints have been developed, most of which typically fall into one of two categories: notch-type joints or leaf spring joints[19]. Notch-type flexible joints have been used by HOWELL and MIDHA[20] to design PRB compliant mechanisms. Leaf springs can also be applied to create a large types of compliant joints[19].

The advantages gained from using compliant joints are offered at the cost of several disadvantages, including limited range of motion, reduced fatigue life and high stress concentration. They must be taken into account when designing compliant mechanisms. The range of motion of a flexible segment is limited by the permissible stresses in the material. The flexible part returns to its original shape and size after the load is removed, providing that the elastic limit is not exceeded. Yielding begins when the yield stress is reached at any point within the segment where elastic deformation becomes plastic deformation. Then flexure behavior due to yielding would be unstable and unpredictable. In actual compliant mechanisms beams can be found in an infinite variety of sizes, shapes and orientations. There are several familiar segments assigned by HOWELL[1], i.e., small-length flexural pivot, fixed-pinned segment, fixed-guided segments, initially curved cantilever beam and pinned-pinned beam. In intuition, the deformation of a corrugated beam is larger than a straight beam or an initially curved beam when the same load is applied. If the spans are same, the corrugated cantilever beam will have a longer centerline which will increase the actual length of beam to deform. To the best of authors' knowledge, there is no simple yet rigorous method to calculate these. This paper introduces an analytic model that provides a simple and generic solution for approximating the large nonlinear deflection of corrugated cantilever beam-based flexure configuration. The accuracy of the proposed model is also investigated. Section 2 outlines PRB model of corrugated beam unit. The overall deflection of a periodically corrugated beam is approximated in section 3. The accuracy of the analytical method is verified by finite element analysis software in section 4. A compliant rotational joint based on corrugated beam is designed in section 5 while some concluding remarks are given in section 6.

2 PRB Model of Corrugated Cantilever Beam Unit

According to Euler-Bernoulli beam theory, the angle of deflection in a simple cantilever beam can be described using the following equation: $\theta=\boldsymbol{M}L/EI$. Here, θ is deflection angle at the free end of a cantilever beam, L is span of cantilever beam, $\boldsymbol{M}$ is the bending moment, E is the elastic modulus and I is the moment of inertia. The deflection at any point along the span can be calculated as long as the material in question has not reached its elastic limit. From Euler-Bernoulli beam theory it follows that the span L and moment of inertia I are the most determining factors. In order to obtain a large deflection angle without changing the material, we have to increase the value of the moment or length. Provided that its length in longitudinal direction is constant, in order to increase L equivalently for large deflection, straight beam can be transformed into corrugated one. Corrugated beam is composed of beam units, namely the blue part shown in Fig. 1. For a periodically corrugated beam, each repeated unit consists of a straight and a semi-circular segment. The definition of parameters is shown in Fig. 1.

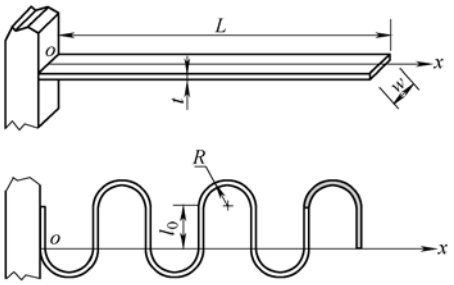

Fig. 1. Straight cantilever beam and corrugated cantilever beam

Fig. 2 gives a maximum deformation comparison of two types of cantilever beams: straight cantilever beam and corrugated cantilever beam. Both the beams have the same span in the longitudinal direction and the same load on free end. The deformation analysis is carried out using finite element analysis software. Obviously under the same conditions, the maximum deformation of corrugated beam is greater than a straight one.

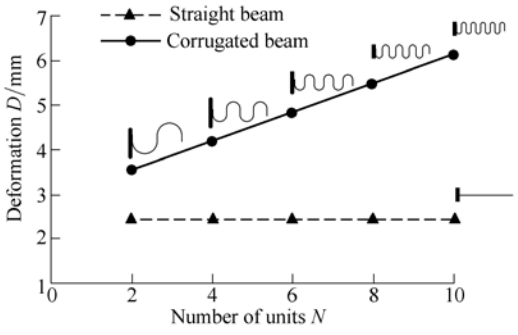

Fig. 2. Comparison of maximum deformation of straight beam and corrugated cantilever beams

2.1 PRB model of semi-circular beam

At a certain angle range, when the free end of flexible cantilever beam is subjected to moment, its deformation trajectory closes to a segment arc of a certain radius. Thus the deformation trajectory of semi-circular beam can be solved through parameter approximation[1].

Fig. 3 shows the pseudo-rigid body model for semi-circular cantilever beam, where γ is the characteristic radius factor. Product γl is characteristic radius, where l is the total length of the beam. Θ is called the pseudo-rigid-body angle. Transform coefficient c_θ describes

the relationship between the pseudo-rigid-body angle and the deformation angle θ_1 of the free end. Taking the initially curved cantilever beam into account, the length of pseudo-rigid-body link is defined as ρl, where ρ is a function of γ and the curvature. The initial coordinates of beam end are (a_i, b_i) and the coordinates of characteristic pivot are $(l(1-\gamma), R-\sqrt{R^2-l^2(1-\gamma)^2})$.

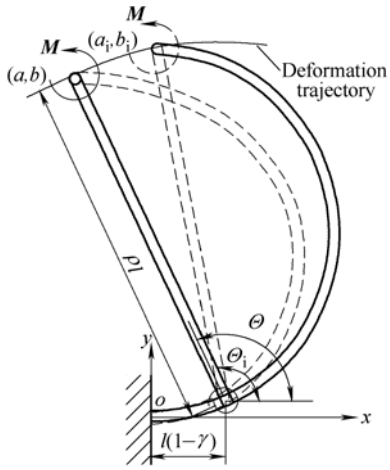

Fig. 3. Pseudo-rigid body model of semi-circular beam

Pseudo-rigid-body angle can be written as

$$\Theta=\pi-\arctan\frac{b_i-R+R-\sqrt{R^2-l^2(1-\gamma)^2}}{a_i-(1-\gamma)}+\frac{12Ml}{c_\theta Ewt^3}, \quad (1)$$

where w is the width of the beam, t is its thickness. And γ=0.734 6, c_θ=1.516 4. The coordinates of semi-circular beam end (a_c, b_c) are given by

$$\begin{cases} a_c=l(1-\gamma+\rho\cos\Theta), \\ b_c=l\rho\sin\Theta+R-\sqrt{R^2-l^2(1-\gamma)^2}, \end{cases} \quad (2)$$

where ρ is given by

$$\rho=\left\{\left[\frac{a_i}{l}-(1-\gamma)\right]^2+\left(\frac{b_i-R-\sqrt{R^2-l^2(1-\gamma)^2}}{l}\right)^2\right\}^{\frac{1}{2}}. \quad (3)$$

Then Eq. (2) can be rewritten as

$$\begin{cases} a_c=l(1-\gamma)+\sqrt{2R^2+2R\sqrt{R^2-l^2(1-\gamma)^2}}\cdot \\ \quad \cos\left[\pi-\arctan\dfrac{R+\sqrt{R^2-l^2(1-\gamma)^2}}{l(1-\gamma)}+\dfrac{12Ml}{c_\theta Ewt^3}\right] \\ b_c=\sqrt{2R^2+2R\sqrt{R^2-l^2(1-\gamma)^2}}\cdot \\ \quad \sin\left[\pi-\arctan\dfrac{R+\sqrt{R^2-l^2(1-\gamma)^2}}{l(1-\gamma)}+\dfrac{12Ml}{c_\theta Ewt^3}\right]+ \\ R-\sqrt{R^2-l^2(1-\gamma)^2}. \end{cases} \quad (4)$$

2.2 Equations for coordinates of straight cantilever beam

Consider the cantilever beam with moment ***M*** applied to the free end, as shown in Fig. 4. The equations for coordinates of beam end has been presented in[1]. The equations for coordinates of beam end can be expressed as

$$\begin{cases} a_s'=l_0\dfrac{\sin\theta_0}{\theta_0}, \\ b_s'=l_0\dfrac{1-\cos\theta_0}{\theta_0}. \end{cases} \quad (5)$$

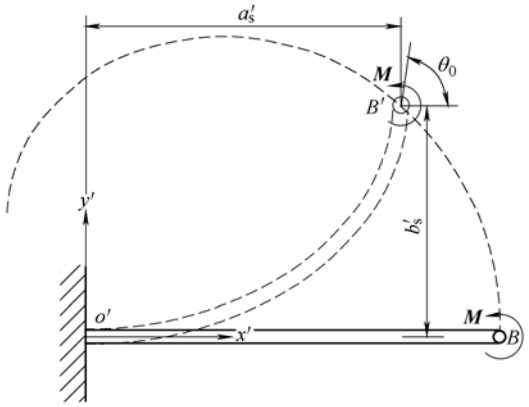

Fig. 4. Flexible cantilever beam with a moment applied to the free end

The deflected angle of the beam end, θ_0, is found by $\theta_0=\boldsymbol{M}l_0/EI$.

2.3 Equations for coordinates of beam unit

There are 4 types of beam units as shown in Fig. 5(a) to Fig. 5(d), which are the basic components of the corrugated beam. And their difference lies on orientations and moment directions.

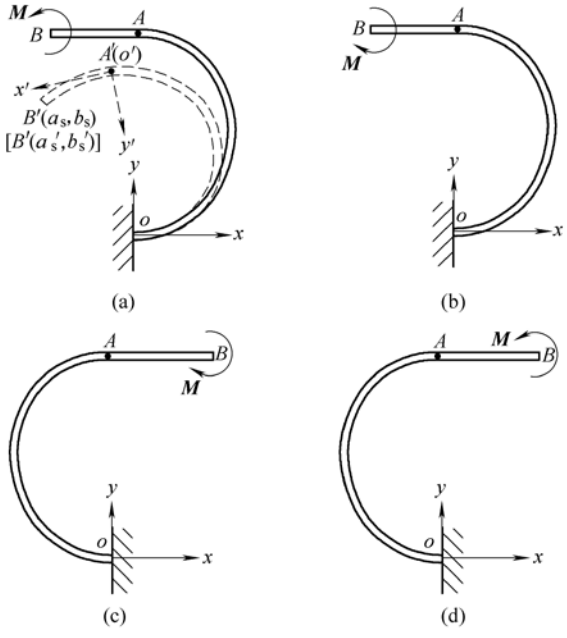

Fig. 5. Beam units with different orientations and moment directions

The deflected beam end coordinates (a_1, b_1) of these units can be expressed by the superimposed deformation of its two segments. The coordinates of straight beam end in the original coordinate system are (a_s, b_s), and the coordinate transformation formula is as follows:

$$\begin{cases} a_s = \sqrt{a_s'^2 + b_s'^2}\cos\left(\pi + \arctan\dfrac{b_s'}{a_s'} + \theta_1\right), \\ b_s = \sqrt{a_s'^2 + b_s'^2}\sin\left(\pi + \arctan\dfrac{b_s'}{a_s'} + \theta_1\right). \end{cases} \tag{6}$$

Equations for coordinates of beam end in Fig. 5(a) (a_1, b_1) can be written as follows:

$$\begin{cases} a_1 = a_c + \dfrac{Ewt^3}{12M}\sqrt{2-2\cos\dfrac{12Ml_0}{Ewt^3}}\cdot \\ \qquad \cos\left(\pi + \arctan\dfrac{1-\cos\dfrac{12Ml_0}{Ewt^3}}{\sin\dfrac{12Ml_0}{Ewt^3}} + \dfrac{12Ml_0}{Ewt^3}\right), \\ b_1 = b_c + \dfrac{Ewt^3}{12M}\sqrt{2-2\cos\dfrac{12Ml_0}{Ewt^3}}\cdot \\ \qquad \sin\left(\pi + \arctan\dfrac{1-\cos\dfrac{12Ml_0}{Ewt^3}}{\sin\dfrac{12Ml_0}{Ewt^3}} + \dfrac{12Ml_0}{Ewt^3}\right). \end{cases} \tag{7}$$

The equations are similar for any of the other units shown in Fig. 5(b) to Fig. 5(d).

3 Evaluation of Corrugated Cantilever Beam with a Pure Moment Loading

When a pure moment loading is applied to a fixed-pinned corrugated beam at the free end, ***M*** is constant along the beam centerline. If it is assumed that the corrugated beam behaves elastically for the moment loading, the resulting final deflection of the loaded beam is simply the sum of the deflections of all units. Therefore, the motion of the system may be interpreted as the superposition of the motion of N single units. Fig. 6 shows a PRB serial chain for modeling a corrugated beam subject to a moment. The modal approach allows to get physical insight about the motion of the corrugated beam.

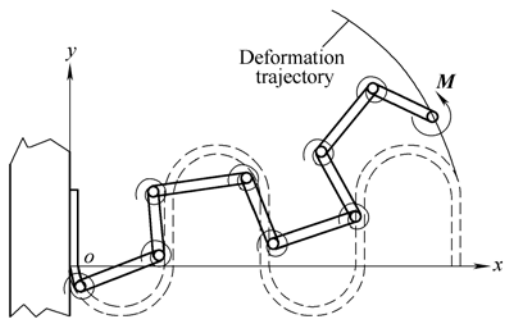

Fig. 6. Pseudo-rigid-body serial chain for a corrugated beam subjected to a moment

Suppose the coordinates of beam end shown in Fig. 5(b) are (a_1, b_1), and let $m=(a_1^2+b_1^2)^{0.5}$, $n=(a_2^2+b_2^2)^{0.5}$, $p=\arctan(b_1/a_1)$, $q=\arctan(b_2/a_2)$, $\theta=\theta_0+\theta_1$. The present method computes the coordinates of corrugated beam end via superimposition and coordinates transformation. By preceding analysis, equations for coordinates of beam units are given. For corrugated cantilever beam with N units, coordinates of its end (a_N, b_N) can be derived as follows:

$$\begin{cases} a_N = a_1 + m\{\cos(\pi+p+2\theta)+\cos(\pi+p+4\theta)+ \\ \qquad \cos(\pi+p+6\theta)+\cdots+\cos[\pi+p+(N-2)\theta]\}+ \\ \qquad n\{\cos(\pi+q+\theta)+\cos(\pi+q+3\theta)+ \\ \qquad \cos(\pi+q+5\theta)+\cdots+\cos[\pi+q+(N-1)\theta]\}, \\ b_N = b_1 + m\{\sin(\pi+p+2\theta)+\sin(\pi+p+4\theta)+ \\ \qquad \sin(\pi+p+6\theta)+\cdots+\sin[\pi+p+(N-2)\theta]\}+ \\ \qquad n\{\sin(\pi+q+\theta)+\sin(\pi+q+3\theta)+ \\ \qquad \sin(\pi+q+5\theta)+\cdots+\sin[\pi+q+(N-1)\theta]\}, \end{cases} \tag{8}$$

when N is an even number, and

$$\begin{cases} a_N = a_1 + m\{\cos(\pi+p+2\theta)+\cos(\pi+p+4\theta)+ \\ \qquad \cos(\pi+p+6\theta)+\cdots+\cos[\pi+p+(N-1)\theta]\}+ \\ \qquad n\{\cos(\pi+q+\theta)+\cos(\pi+q+3\theta)+ \\ \qquad \cos(\pi+q+5\theta)+\cdots+\cos[\pi+q+(N-2)\theta]\}, \\ b_N = b_1 + m\{\sin(\pi+p+2\theta)+\sin(\pi+p+4\theta)+ \\ \qquad \sin(\pi+p+6\theta)+\cdots+\sin[\pi+p+(N-1)\theta]\}+ \\ \qquad n\{\sin(\pi+q+\theta)+\sin(\pi+q+3\theta)+ \\ \qquad \sin(\pi+q+5\theta)+\cdots+\sin[\pi+q+(N-2)\theta]\}, \end{cases} \tag{9}$$

when N is an odd number.

Many parametric studies were performed on the analytical model of the corrugated beam to create a catalog of graphs that serves as a quick look at the characteristics of the beam. These charts are presented to the designer to be used in an iterative fashion when designing beams. Six dual-parameter studies were done with the corrugated beam, represented by 3D surface plots of the output variables. The six studies consisted of three groups to evaluate: coordinates of its end (X and Y), largest deflection. In each of these studies, the following two combinations of parameters were inspected: straight segment length and number of units, and thickness and width.

The first quantity considered reflects the desired motion of the beam: coordinates of its end. Fig. 7 and Fig. 8 plot the coordinates of the free end of corrugated beam as to visualize Eqs. (8) and (9). In either figure, the span (L) is the same. Fig. 7 shows the combined effects of straight segment length and number of units on the coordinates. Note that in Fig. 7 the length of straight beam has a linear effect on both X and Y while the number of units has a positive correlation only with X.

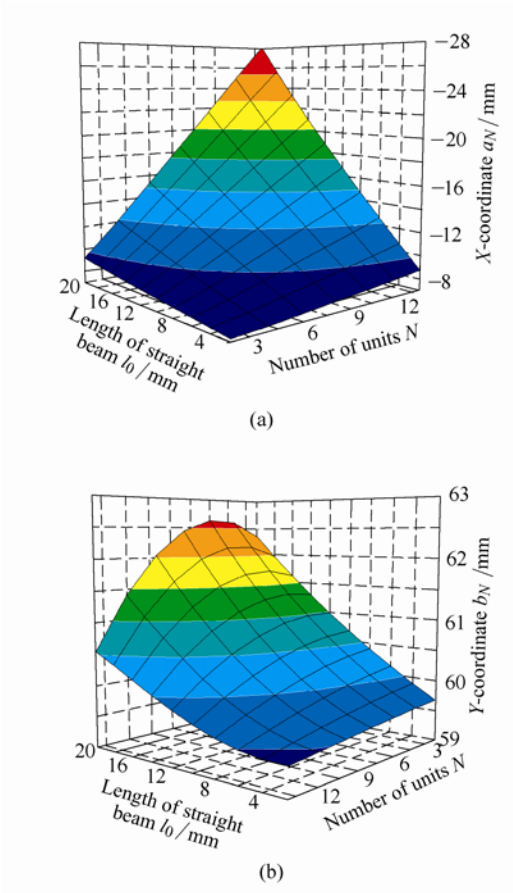

Fig. 7. Position of the free end (N & l_0)

Fig. 8 shows the combined effects of beam thickness and width. Beam width has a nonlinear effect on coordinates for a given beam length. And also beam length nonlinearly increases the coordinates for a given width.

To maximize the desired compliance, deflections of its end, illustrated in Fig. 9, must be maximized. Fig. 9(a) shows the combined effects of straight beam length and number of units on the largest deflection. Beam length has a linear effect on deflections for a given number of units. And, the number of units also linearly increases the deflections for a given length. It is reasonable that the compliance increases linearly with respect to the centerline length of the corrugated beam ($N \cdot l_0 + L \cdot \pi/2$). Fig. 9(b) shows the combined effects of beam width and thickness on the largest deflection. It indicates that the deflection increases nonlinearly with respect to width when the thickness is constant and vice versa.

4 Comparison of the PRB Model with the Numerical Result

In the previous section, the deflection of fixed-Pinned corrugated beam end is found by analytical methods. The method will be compared with numerical method in order to estimate the accuracy of analytical method. The verification experiment is completed with Ansys. The material used for the corrugated beam is 60Si2Mn. The Young's modulus assumed is 206 GPa with Poisson's ratio of 0.29 and yield strength of 1 176 MPa.

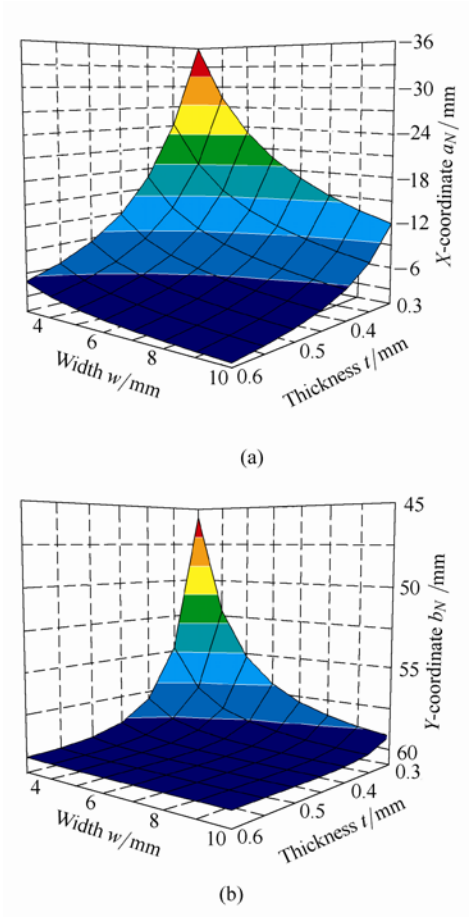

Fig. 8. Position of the free end (t & w)

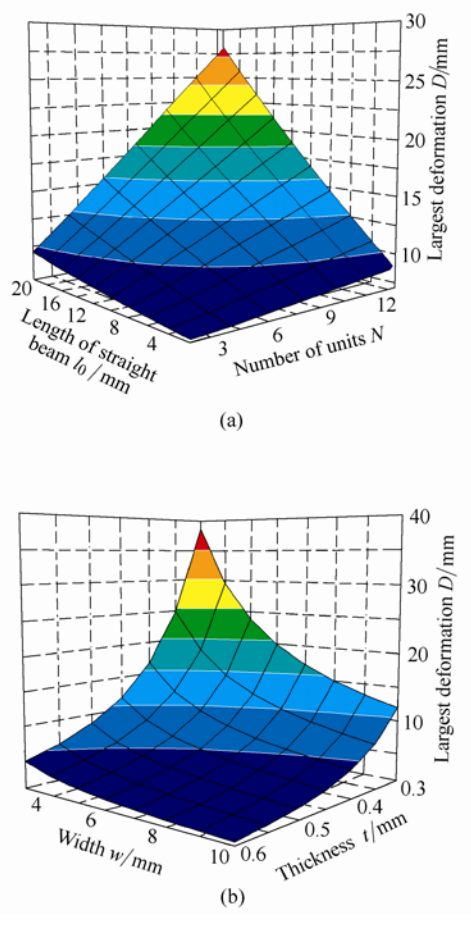

Fig. 9. Deflection of corrugated cantilever beam

First, the deflections of the four units shown in Fig. 5 are testified by analytic and numerical methods. Errors of these individual units accumulate to determine the overall error in the final corrugated beam, and determine whether the deformed trajectory derived by the PRB model remains feasible or not. The analytical and simulation values are tabulated in Table 1. The results listed in Table 1 show that the largest error is 2.8% and within acceptable limit.

Table 1. Analytical and simulation values for units shown in Fig. 5 (M=38 N • mm, R=l_0=8.465 mm)

	Fig. 5(a)	Fig. 5(b)	Fig. 5(c)	Fig. 5(d)
Analytical value V_a/mm	9.437 9	8.685 9	8.687 0	9.436 7
Simulation value V_s/mm	9.704 8	8.560 0	8.560 0	9.704 8
Relative error δ/%	2.8	1.5	1.5	2.8

Then the accuracy of the analytical method with different dimension parameters was investigated. Changes in the dimensions of the unit shown in Fig. 5(a) during a test were used to measure its deformation. The meaning of parameters is the same as in Fig. 1. The solution set under different loading conditions is shown in Fig. 10 where the numerical results of the deformation are shown with dotted line and the analytical results with solid line. The plot shows that the analytical and simulation curves can hardly be distinguished, as they overlap over most of the domain. The preliminary test series confirm the feasibility of the PRB model.

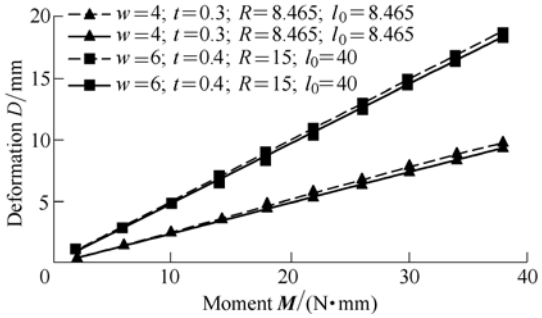

Fig. 10. Comparison of the analytical values and simulation values of the beam unit

The deflection of the corrugated beam is a function of parameters of beam units and number of units. The recursive Eqs. (8) and (9) were computed, and deflection was determined. The relative deviations under different loading and beam parameters from the numerical results are plotted in Fig. 11. The results in Fig. 11 show that the largest deviation is about 6% and within acceptable limits. These results suggest that error of a single beam unit is reasonably low. But the error will be accumulated with the increase in number of beam units. The overall error fluctuates within a narrow range and this leads to the fact that the proposed PRB model can contribute to analyze the deformation of corrugated beam. And it's feasible to solve the deformation trajectory of the free end of corrugated beam by pseudo-rigid-body model.

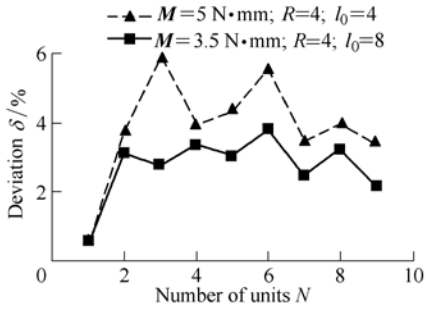

Fig. 11. Beam errors under different loading conditions

5 Application in Flexible Joint

The flexible rotational joint is a new type of assembly free hinge with a flexible joint alternative to revolute joint in traditional rigid body using its own elastic deformation rather than the movement of rigid components to transform the force, movement or energy. It overcomes friction, noise and vibration of the rigid hinge. Corrugated cantilever can be used to design a flexible rotational joint, as shown in Fig. 12.

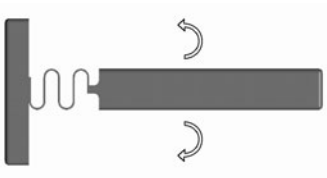

Fig. 12. Corrugated beam-type flexible rotational joint

In the last 50 years, many rotational flexible joints have been researched and developed, most of which are considered as notch-type joints (Figs. 13(a), 13(b)) and leaf springs (Fig. 13(c)). Notch-type flexible joints (fillet joints) have become well understood by many researchers and designers. Today, notch-type joint assemblies are widely used for high-precision, small-displacement mechanisms. These joints have also been applied to develop the field of pseudo-rigid-body compliant mechanisms. However, their rotation range is limited[19] because of the permissible stresses and strains in the material.

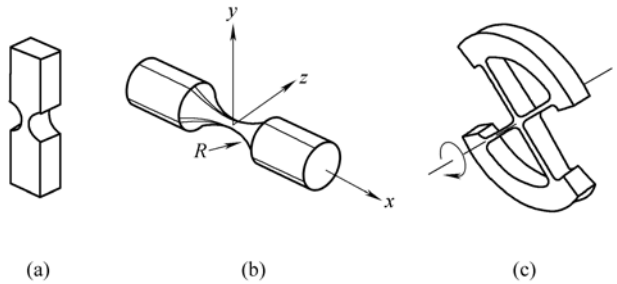

Fig. 13. Traditional flexible joints

In order to get equal end deflection angle and equal maximum stress to straight one, the thickness of the corrugated beam should be increased and accordingly the moment load. This leads to increase in its rotational

stiffness and its easy processing. So this flexible rotational joint has following advantages: high load performance, high manufacturability, and large rotation range. Fig. 14 gives a comparison of three different rotational joints and illustrates how joint geometry has had a distinct impact on the rotation range. Rotational joints in Fig. 14 are all subjected to the same moment.

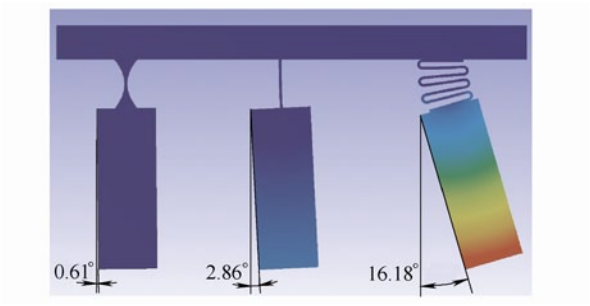

Fig. 14. Comparison of rotation range of the corrugated beam-type flexible rotational joint and traditional flexible joints

In order to obtain the largest possible deflection angle, the corrugated beam should be optimized. While Fig. 9(a) suggests long straight beam lengths, and large number of beam units for maximal compliance, these conflict with the requirements for non-contact between two adjacent beam units. After the parameters I, L and l_0 are defined, it's rather difficult to confirm number of units N by analytical method. With the assistance of finite element analysis tools, all will be convenient. The maximum moment ($\boldsymbol{M}_{\max}$) can be obtained from the equation $\sigma=\boldsymbol{M}_c/I$. Let $\boldsymbol{M}_c$ be the moment that will cause two adjacent beam units to contact. Assign N and find out $\boldsymbol{M}_c$. Adjust N until $\boldsymbol{M}_c$ is equal (or close) to $\boldsymbol{M}_{\max}$. By the above method, the number of units can be determined as 5 when I=0.032 mm^4, l_0=5 mm and $\boldsymbol{M}_{\max}$=84.93 N • mm, as shown in Fig. 15. And the largest deflection angle can be obtained. However, in practical applications, sufficient margin should be kept against contact so as to improve its durability and accuracy when the number of units is determined.

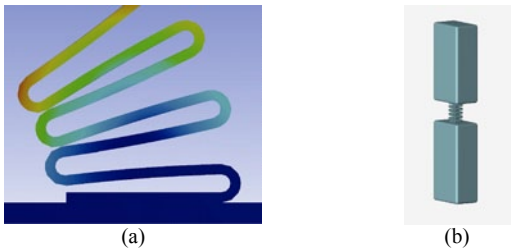

(a) (b)

Fig. 15. Corrugated beam-type flexible rotational joint with optimal structure

6 Conclusions

(1) Pseudo-rigid-body model for the corrugated beam tallies with the simulation results.

(2) As a new type of flexible components, corrugated beam greatly compensates the lack of straight beam in obtaining large deformation.

(3) Due to the outstanding advantages of corrugated beam, it can be used as flexible component in precision measurement and localization, MEMS, and so on.

References

[1] HOWELL L L. *Compliant mechanisms*[M]. New York: McGraw-Hill, 2001.

[2] KOTA S, JOO J, LI Z, et al. Design of compliant mechanisms: Applications to MEMS[J]. *Analog Integrated Circuits and Signal Processing*, 2001, 29(1): 7–15.

[3] PERAI S. Methodology of compliant mechanisms and its current developments in applications: a review[J]. *American Journal of Applied Sciences*, 2007, 4(3): 160–167.

[4] MCCARTHY J M. 21st century kinematics: synthesis, compliance, and tensegrity[J]. *JMR Editorial*, 2011, 3(2): 020201.

[5] BENDSOE M P, KIKUCHI N. Generating optimal topologies in structural design using a homogenization method[J]. *Computer Methods in Applied Mechanics and Engineering*, 1988, 71(2): 197–224.

[6] HAGISHITA T, OHSAKI M. Topology optimization of trusses by growing ground structure method[J]. *Structural and Multidisciplinary Optimization*, 2009, 37(4): 377–393.

[7] WANG Michael Yu, WANG Xiaoming, GUO Dongming. A level set method for structural topology optimization[J]. *Computer Methods in Applied Mechanics and Engineering*, 2003, 192(1): 227–246.

[8] WANG Nianfeng, TAI K. Design of grip-and-move manipulators using symmetric path generating compliant mechanisms[J]. *Journal of Mechanical Design, Transactions of the ASME*, 2008, 130: 112305.

[9] WANG Nianfeng, TAI K. Design of 2-DOF compliant mechanisms to form grip-and-move manipulators for 2D workspace[J]. *Journal of Mechanical Design, Transactions of the ASME*, 2010, 132: 031007.

[10] WANG Nianfeng, YANG Yaowen. Structural design optimization subjected to uncertainty using fat Bezier curve[J]. *Computer Methods in Applied Mechanics and Engineering*, 2009, 199(1): 210–219.

[11] WANG Nianfeng, TAI K. Target matching problems and an adaptive constraint strategy for multiobjective design optimization using genetic algorithms[J]. *Computers & Structures*, 2010, 88(19): 1 064–1 076.

[12] WANG Nianfeng, ZHANG Xianming. Compliant mechanisms design based on pairs of curves[J]. *SCIENCE CHINA Technological Sciences*, 2012, 55(8): 2 099–2 106.

[13] XIAO Shunli, LI Yangmin, ZHAO Xinhua. Design and analysis of a novel micro-gripper with completely parallel movement of gripping arms[C]//*6th IEEE Conference on Industrial Electronics and Applications (ICIEA)*, Beijing, China, 2011: 2 127–2 132.

[14] WILCOX D L, HOWELL L L. Fully compliant tensural bistable micromechanisms(FTBM)[J]. *Journal of Microelectromechanical Systems*, 2005, 14(6): 1 223–1 235.

[15] CHEN Guimin, XIONG Botao, HUANG Xinbo. Finding the optimal characteristic parameters for 3R pseudo-rigid-body model using an improved particle swarm optimizer[J]. *Precision Engineering*, 2011, 35(3): 505–511.

[16] MATTSON C A, HOWELL L L, MAGLEBY S P. Development of commercially viable compliant mechanisms using the pseudo-rigid-body model: case studies of parallel mechanisms[J]. *Journal of Intelligent Material Systems and Structures*, 2004, 15(3): 195–202.

[17] SU X P, YANG H S. Two-stage compliant microleverage mechanism optimization in a resonant accelerometer[J]. *Structural and Multidisciplinary Optimization*, 2001, 22(4): 328–334.

[18] SU H J. A pseudorigid-body 3R model for determining large

deflection of cantilever beams subject to tip loads[J]. *Journal of Mechanisms and Robotics*, 2009, 1: 021008.

[19] TREASE B P, MOON Y M, KOTA S. Design of large-displacement compliant joints[C]//*27th Biennial Mechanisms and Robotics Conference*, Montreal, Canada, September 29–October 2, 2002: 65–76.

[20] HOWELL L L, MIDHA A. A method for the design of compliant mechanisms with small-length flexural pivots[J]. *Journal of Mechanical Design*, 1994, 116: 280–290.

Biographical notes

WANG Nianfeng, born in 1977, is currently an associate professor at *South China University of Technology, China.* He received his PhD degree from *Nanyang Technological University, Singapore*, in 2008. His research interests include compliant mechanism, structural optimization and robotics.
Tel: +86-20-87110059; E-mail: menfwang@scut.edu.cn

LIANG Xiaohe, born in 1989, is currently a master candidate at *South China University of Technology, China*. His research interests include compliant mechanism, precision equipment.
E-mail: 746155882@qq.com

ZHANG Xianmin, born in 1964, is currently a professor at *South China University of Technology, China.* He received his PhD degree from *Beihang University, China*, in 1997. His research interests include mechachonics engineering, compliant mechanism.
Tel: +86-20-87110059; E-mail: zhangxm@scut.edu.cn